Journal of Nano- and Electronic Physics
Vol. **7** No 2, 02007(7pp) (2015)

Журнал нано- та електронної фізики
Том **7** № 2, 02007(7cc) (2015)

Optimization of Band Gap and Thickness for the Development of Efficient *n-i-p*$^+$ Solar Cell

A. Belfar*, B. Amiri, H. Aït-kaci

Laboratory of plasma physics, Conductor Materials and their Applications, Faculty of Physics, Oran University of Sciences and Technology Mohamed Boudiaf USTO-MB, BP1505 Oran, Algeria

(Received 05 February 2015; revised manuscript received 05 June 2015; published online 10 June 2015)

By using an electrical-optical AMPS-1D program (One Dimensional Analysis of Microelectronic and Photonic structures), a *n-i-p* type solar cell, based on hydrogenated amorphous silicon (a-Si : H) and hydrogenated nanocrystalline silicon oxide (nc-SiO$_x$: H) has been investigated and simulated. The numerical analysis describes the modeling of the external cell performances, like, the short-circuit current (J_{SC}), the open circuit voltage (V_{OC}), the fill factor (*FF*) and efficiency (E_{ff}) with the oxygen content in the *p-nc*-SiO*x* : H window layer by varying its mobility band gap (E_g) associated simultaneously to the effect of the absorber layer (*i-a*-Si : H) thickness. Also, the *i-a*-Si : H absorber layer band gap was optimized. The simulation result shows that the V_{OC} depend strongly on the band offset (ΔE_V) in valence band of p-side. But, V_{OC} does not depend on the thickness of the intrinsic layer. However, V_{OC} increases when the energy band gap of the intrinsic layer is higher. It is demonstrated that the highest efficiency of 10.44 % (J_{SC} = 11.67 mA/cm^2; *FF* = 0.829; V_{OC} = 1070 mV) has been obtained when values of *p-nc*-SiO*x* : H window layer band gap, *i-a*-Si : H absorber layer band gap and *i-a*-Si : H absorber layer thickness are 2.10 eV, 1.86 eV, and 550 nm, respectively.

Keywords: Solar cells, *a*-Si : H, Thickness, Window layer, *nc*-SiO*x* : H; Simulation, AMPS-1D.

PACS numbers: 73.40.Lq, 78.20.Bh

1. INTRODUCTION

The cost of manufacturing cells in thin layers based on amorphous silicon (a-Si : H) is smaller and present a lot of opportunities for deposition on different substrates types (rigid, flexible, lightweight). All the works carried out in this direction, try to develop new manufacturing processes and invent new designs in order to improve the solar cells performances with a low production cost [1-4]. Many techniques can be used to improve the conversion efficiency of a solar cell. On the one hand, the interfaces between the materials of the window, the electrodes and the intrinsic region (active area) must be of good quality. On the other hand, a wide band gap semiconductor material, *p*-type, may be used as window layer in order to improve light transmission. This same layer must be of high conductivity to increase the electrical potential in the structure and reduce the effects of the series resistance [5]. This leads to a better match between the different layers of the structure. In this work there is a window layer based on nanocrystalline silicon oxide (*p-nc*-SiO*x* : H), with a gap which can vary from 2 eV to 2.25 eV, depending on the dosage of oxygen atoms. It is found in the experiment by Rémi Biron et al. [6], the incorporation of oxygen in the H-diluted p-layer leads to the linear widening of the band gap. However, when the content of oxygen varying from 0 % to 36 % the gap E_g of the *p-n*-SiO*x* : H layer increase from 1.81 to 2.29 eV [6]. Pingate et al. reported an increase in efficiency in a cell based on *μc*-Si and with a *p-nc*-SiO*x* layer [7]. In a study conducted by Pingate et al. on the electrical and optical characteristics of the layers of *p-nc*-SiO*x*, it has been revealed that there is a clear separation of phases in these films between rich in silicon (Si) and those rich in oxygen (O) [7]. It was also shown that the microstructure of *nc*-SiO*x* *p*-layers can improve the efficiency of Micromorph cells (Tandem). In particular, a layer of *p-nc*-SiO*x* improve the contact quality by reducing the effect of the roughness of the front electrode over the performances of cells, either in single or Micromorph configuration [8]. This work, consists in a study of the performances of a solar cell at single *n-i-p* design, using hydrogenated amorphous silicon (*i-a*-Si : H) as active layer and *p-nc*-SiO*x* : H as a window layer. On one hand, our purpose is to study simultaneously the effect of the active layer thickness associated to the variation in the mobility band (E_g) of window layer on the cell performances. On the other hand it was achieved the extraction of physical parameters characterizing each layers constituting the structures. Also, the effect of absorber layer band gap was studied.

2. DISCRIPTION OF THE SIMULATED STRUCTURE

We have considered a model based on hydrogenated amorphous silicon (*a*-Si : H) and nanocrystalline silicon oxide to design our simulated *n-i-p*$^+$ substrate structure. These tow materials were used by other authors to realize experimentally a *p-i-n* superstrate solar cells by RF-PECVD technology (Radio Frequency Plasma-Enhanced Chemical Vapor Deposition) [1, 2]. The *n-i-p*$^+$ characterized device contain a 10 nm thick front p-doped layer of *nc*-SiO*x* : H, a 10 nm thick back *n*-doped layer of *a*-Si : H, an intrinsic *a*-Si : H absorber layer of variable thickness. An intrinsic buffer layer based on carbon hydrogenated amorphous silicon (*i-a*-SiC : H) with a thickness of 3 nm, has been incorporated between the p-window and the absorber *i*-layer. Our structue was considred deposited on a metal substrate which functions as a back contact. For the front contact, a 80 nm thick TCO (Transparent Conducting Oxide) layer has been deposited on the p-side (Fig. 1).

* a_belfar@hotmail.com

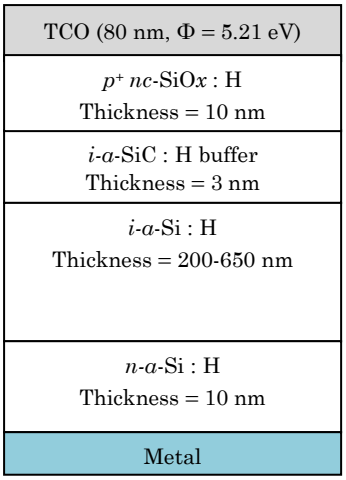

Fig. 1 – Shematic diagram of the *n-i-p*⁺ simulated solar cell

3. SIMULATION MODEL FOR AMORPHOUS (*a*-SI : H) AND HYDROGENATED NANO-CRYSTALLINE SILICON OXIDE (*nc*-SIO$_X$: H)

The AMPS-1D program, used in this study, solves Poisson's equation coupled to electrons and holes continuity equations, at each position throughout the device [9]. The resolution uses finite differences and the Newton-Raphson methods. AMPS-1D simulates device operation by taking into account the Shockley-Read-Hall recombination statistics. The numerical simulation also requires a model for the density of trap states in the structure. In the simulation presented here, the density of states (DOS) for the localized states in the mobility gap of *a*-Si : H and *nc*-SiO*x* : H materials, it has been assumed that there are both exponential Urbach tail states and Gaussian-shaped midgap states (associated to silicon dangling bonds). The tail states consist of a donor tail coming out of the valence band and an acceptor tail coming out of the conduction band. The valence and the conduction band tail states have an exponential distribution in energy and are usually given as follows:

$$g_A(E) = G_{AO} \exp\left(\frac{E-E_C}{E_A}\right), \quad (1)$$

$$g_D(E) = G_{DO} \exp\left(\frac{E_V-E}{E_D}\right), \quad (2)$$

Where $G_{AO}(E)$ and G_{DO}(iE) are the densities per energy range for tail states at the band edge energies E_V and E_C, respectively; and E_A and E_D are characteristic parameters for the conduction and valence band tail states, respectively.

While the midgap states are composed of an acceptor Gaussian and donor Gaussian described by:

$$g_A(E) = N_{AG} exp\left\{-\frac{1}{2}\left[\frac{E-E_{ACPG}}{W^2_{DSAG}}\right]\right\} \quad (3)$$

$$g_D(E) = N_{DG} exp\left\{-\frac{1}{2}\left[\frac{E-E_{DONG}}{W^2_{DSDG}}\right]\right\} \quad (4)$$

Where E_{ACPG} and E_{DONG} are the peak energy position, N_{AG} and N_{DG} are the effective density of statesand W_{DSAG} and W_{DSDG} are the standard energy deviation of the Gaussian acceptor and donor levels, respectively. The peak energies for the Gaussian donor-and acceptor-like states are measured from the conduction and valence bands, respectively. Since the gap states can exchange carriers with the conduction and valence bands, capture cross-sections for each state must be specified for both electrons and holes [6].

4. ELECTRICAL AND OPTICAL INPUT PARAMETERS FOR SIMULATION

The calculation using the AMPS-1D program requires input parameters such as surface recombination velocities, barrier heights, power density of the radiation and characteristics of the layers forming the structure to simulate.

For electrons and holes, we used the value of 10^7 cm/s as speeds of surface recombination [10, 11]. According to Arch et al. [12], the barrier height for electrons (φ_{b0}) at front contact (TCO / *p*-layer) is related to the electron affinity (χ_e) of *p*-layer and the work function ($\Phi_{w,\,front}$) of TCO, by:

$$\varphi_{b0} = \Phi_{w,\,front} - \chi_e \,|_{x=0} \quad (5)$$

In our case, the values of 5.21 eV and 3.76 eV are used for $\Phi_{w,\,front}$ and χ_e, respectively. These values leads to a value of φ_{b0} equal to 1.45 eV. The back contact barrier height φ_{bL} (*n* layer / metal) is chosen equal to 0.21 eV. φ_{bL} represents the activation energy of the n-layer [13]. In hydrogenated nanocrystalline oxide layer, the values of 5 $cm^2 \cdot V^{-1} \cdot S^{-1}$ and 0.5 $cm^2 \cdot V^{-1} \cdot S^{-1}$ were used, for the electrons (μ_e) and holes (μ_h) mobility, respectively [14]. However, the electron affinity (χ) is assumed different for layers based on *p-nc*-SiO*x* : H and their based on *a*-Si : H. All other electrical parameters used in the simulation are summarized in Table 1.

As a source of illumination, an AM 1.5 solar radiation with a power density of 100 mW/cm^2 was used. The reflection of light at the front face (RF) was set at 0.2. For the back contact we chose the value of 0.6, for retro-reflection (RB). The light absorption coefficient, for the different layers was already incorporated in the AMPS-1D program.

5. SIMULATION RESULTS AND DISCUSSION

5.1 Optimization of *p-nc*-SiO$_X$: H Window Layer Band Gap

In *p-i-n* solar cell, the window layer perform an important role, therefore its band gap define the amount of light achieved the intrinsic layer. However, a wide band gap material is recommended to reduce the losses due to the absorption. Also we konw, that electrons and holes generated in doped layers usually do not contribut to the photocurrent for their short life time. Forthermore, in *p-i-n* single *a*-Si : H based solar cells, *i*-layer thickness is one of the fundamental factors which influence the reduction of material costs and improve collection efficiency. Hence, a simultaneous optimization of *p*-window layer band gap and *i*-absorber layer thickness was performed in order to realize efficient solar cells. During the optimization of *p-nc*-SiO$_X$: H layer band gap and *i-a*-Si : H layer thickness the values of *i-a*-SiC : H buffer, *i-a*-Si : H and n layer band gaps where kept as 1.80 eV,

1.90 eV and 1.75 eV, respectively. The thicknesses of *p*-layer, buffer layer and n layer were kept as 10 nm, 3 nm and 10 nm, respectively. For this, we varying simultaneously the thickness of *i*-*a*-Si : H from 200 nm to 650 nm and the gap of the p-window layer from 2 eV to 2.25 eV. Fig. 2a-d shows the variations of J_{SC}, V_{OC}, *FF* and efficiency with simultaneous variations of *p*-*nc*-SiO$_X$: H window layer band gap and *i*-*a*-Si : H absorber layer thickness. From Fig. 2a, J_{SC} is not affected by *p*-*nc*-SiO$_X$: H window layer band gap variations but J_{SC} increase from 10.55 mA/cm^2 to 12.45 mA/cm^2 with increasing the *i*-layer thickness from 200 nm to 650 nm. This can be attributed to an increase in the quantum efficiency in the whole of wavelengths.

In our case, the values of 5.21 eV and 3.76 eV are used for $\Phi_{w,\,front}$ and χ_e, respectively. These values leads to a value of φ_{b0} equal to 1.45 eV.

The back contact barrier height φ_{bL} (*n* layer / metal) is chosen equal to 0.21 eV. φ_{bL} represents the activation energy of the *n*-layer [13].

In hydrogenated nanocrystalline oxide layer, the values of $5\ cm^2{\cdot}V^{-1}{\cdot}S^{-1}$ and $0.5\ cm^2{\cdot}V^{-1}{\cdot}S^{-1}$ were used, for the electrons (μ_e) and holes (μ_h) mobility, respectively [14]. However, the electron affinity (χ) is assumed different for layers based on *p*-*nc*-SiO*x* : H and their based on *a*-Si : H. All other electrical parameters used in the simulation are summarized in Table 1.

As a source of illumination, an AM 1.5 solar radiation with a power density of 100 mW/cm^2 was used. The reflection of light at the front face (RF) was set at 0.2. For the back contact we chose the value of 0.6, for retro-reflection (RB). The light absorption coefficient, for the different layers was already incorporated in the AMPS-1D program.

The variations of V_{OC} with *p*-*nc*-SiO*x* : H layer band gap where presented in Fig. 2b. We can see that the variations with *i*-*a*-Si : H thickness are not very important for example at *p*-*nc*-SiO*x* : H layer band gap equal to 2.10 eV the V_{OC} decreased from 1015 mV to 990 mV when *i*-*a*-Si : H thickness increased from 200 nm to 650 nm. But, the variations of V_{OC} with *p*-*nc*-SiO*x* : H layer band gap can be found increased initially from 991 mV to1015 mV with the increasing *p*-*nc*-SiO*x* : H layer band gap from 2 eV to 2.10 eV. After, in the band gap range 2.10 eV-2.15 eV, value of V_{OC} remains constant. However beyond 2.15 eV, value of V_{OC} was found to decrease gradually. We have shown the band diagram of *n*-*i*-*p*$^+$ solar cells in Fig. 3a-f in order to understand the variations in V_{OC} with the increasing *p*-*nc*-SiO*x* : H layer band gap.

When the junction field separates the photogenerated *e*-*h* pairs, electrons have to move towards *n*-side through conduction band and holes have to move towards *p*-side through valence band.

Table 1 – Parameters extracted from the simulation for the studied structure at room temperature

Parameters	*nc*-SiO*x* : H (*p*$^+$)	Buffer *a*-SiC : H (*i*)	*a*-Si : H (*i*)	*a*-Si : H(*n*)
ε_r	11.9	11.9	11.9	11.9
L (nm)	10	3	200-650	10
χ (eV)	3.76	3.92	4.00	4.00
E_g (eV)	2-2.25	1.90	1.78-1.90	1.75
E_a (eV)	0.06	0.07	0.40	0.20
N_C (cm^{-3})	1×10^{23}	2×10^{20}	2×10^{20}	2×10^{20}
N_V (cm^{-3})	1×10^{23}	2×10^{20}	2×10^{20}	2×10^{20}
μ_{e-} (cm^{2}V^{-1}S^{-1})	2	2	20	10
μ_{h+} (cm^{2}V^{-1}S^{-1})	0.2	0.2	2	01
N_A (cm^{-3})	1×10^{19}	1×10^{16}	0	0
N_D (cm^{-3})	0	0	0	1×10^{19}
G_{DO} / G_{AO}(cm^{-3}eV^{-1})	2×10^{20}	2×10^{20}	2×10^{21}	2×10^{21}
E_D / E_A (eV)	0.02 / 0.01	0.02 / 0.01	0.05 / 0.03	0.05 / 0.03
σ_{de} (cm^2) (Tails)	1×10^{-15}	1×10^{-15}	1×10^{-15}	1×10^{-15}
σ_{dh} (cm^2) (Tails)	1×10^{-17}	1×10^{-17}	1×10^{-17}	1×10^{-17}
σ_{ae} (cm^2) (Tails)	1×10^{-17}	1×10^{-17}	1×10^{-17}	1×10^{-17}
σ_{ah} (cm^2) (Tails)	1×10^{-15}	1×10^{-15}	1×10^{-15}	1×10^{-15}
N_{DG} (cm^{-3})	1×10^{17}	1×10^{16}	5×10^{15}	5×10^{18}
N_{AG} (cm^{-3})	1×10^{17}	1×10^{16}	5×10^{15}	5×10^{18}
E_{DG} / E_{AG} (eV)	1.50 / 0.98	1.38 / 0.78	1.22 / 0.70	1.22 / 0.70
σ_{de} (cm^2) (Gauss.)	1×10^{-14}	1×10^{-14}	1×10^{-14}	1×10^{-14}
σ_{dh} (cm^2) (Gauss.)	1×10^{-15}	1×10^{-15}	1×10^{-15}	1×10^{-15}
σ_{ae} (cm^2 (Gauss.)	1×10^{-15}	1×10^{-15}	1×10^{-15}	1×10^{-15}
σ_{ah} (cm^2) (Gauss.)	1×10^{-14}	1×10^{-14}	1×10^{-17}	1×10^{-17}

The abbreviations used in this table are the following: ε_r – relative dielectric permittivity, L – film thickness, χ – electron affinity, Eg – energy band gap, μ_e, μ_h – mobility of electrons and holes, N_D, N_A – doping donor and acceptor, N_C, N_V – effective densities of states in the conduction and valence bands, N_{DG}, N_{AG} – Gaussian densities for donor and acceptor states, G_{DO}, G_{AO} – exponential prefactors of donor-like or acceptor-like tail states, E_D, E_A – characteristic energy of the donor-like / acceptor-like tail states, E_{DG} / E_{AG} – donor and acceptor Gaussian peak energy position. σ_{de}, σ_{dh} – Capture cross-section for donor states, *e*, *h* and σ_{ae}, σ_{ah} – Capture cross-section for acceptor states *e*, *h*.

However, when *p-nc*-SiO*x* : H band gap range from 2 eV to 2.10 eV the band offset (ΔE_V) in valence band at *p-nc*-SiO*x* : H / *i-a*-SiC : H buffer layer interface is low Fig. 3a-c, so the photogenerated holes can move easly towards *p*-side and the value of V_{OC} is improved. However, when *p-nc*-SiO*x* : H band gap range from 2.15 eV to 2.25 eV there will be an important band offset (ΔE_V) in valence band of p-side, because band gap of buffer layer is kept as 1.90 eV Fig. 3d-f. This offset creates barrier for holes as they have to move towards *p*-side which increase the recombination rate at *p-nc*-SiO*x* : H / *i-a*-SiC : H interface and lower the V_{OC}. The variations of *FF* with *i-a*-Si : H layer thickness and *p-nc*-SiO*x* : H layer band gap where presented in Fig. 2c. Initially, in the band gap range 2 eV-2.10 eV, value of *FF* remains constant. However beyond 2.10 eV, value of *FF* was found to decrease gradually. In one hand, the decrease of *FF* with increasing *i-a*-Si : H layer thickness from 200 nm to 650 nm can be attributed to the insufficient collection within the *i*-layer. On the other hand, the decrease of *FF* with

increasing *p-nc*-SiO*x* : H layer band gap from 2.10 eV to 2.25 eV is du to the high value of band offset (ΔE_V) in valence band.

Fig. 2d showed the simulated result of efficiency. Firstly, with i-layer thickness variations, the efficiency was found to gradually increase from 9 % to 9.92 % with increasing *i-a*-Si : H layer thickness from 200 nm to 550 nm and becomes constant in the range of 550 nm-650 nm. Secondly, with *p-nc*-SiO*x* : H layer band gap variations, value of efficiency increase gradually from 9.83 % to 9.92 % with increasing *p-nc*-SiO*x* : H band gap from 2 eV to 2.10 eV. However, beyond 2.10 eV value of efficiency drastically decreased from 9.92 % to 8.89 %. Hence, *i-a*-Si : H absorber layer thickness of 550 nm and *p-nc*-SiO*x* : H window layer band gap of 2.10 eV where optimized for obtaining high efficiency for *n-i-p*$^+$ solar cell.

5.2 Optimization of *i-a*-Si : H Absorber Layer Band Gap

The *i*-layer in *n-i-p*$^+$ solar cell acts as absorber layer and absorption of incident light strongly depends on the band gap. Hence, optimization of i-layer band gap was performed in order to realize efficient solar cells. During the optimization of *i-a*-Si : H layer band gap, the values

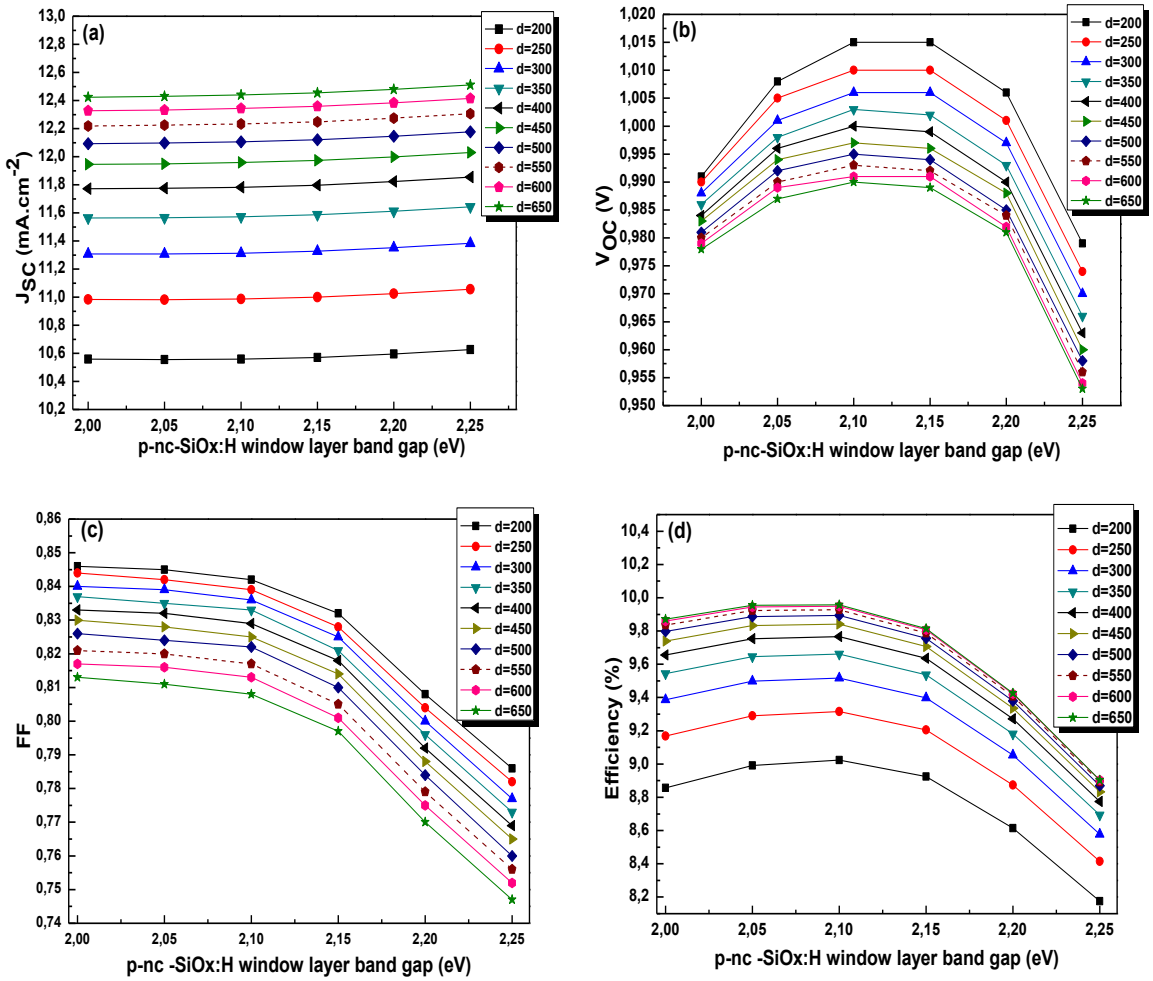

Fig. 2 – Variations of (a) J_{SC}, (b) V_{OC}, (c) *FF* and (d) efficiency with *i-a*-Si : H absorber layer thickness and *p nc*-SiO*x* : H window layer band gap for *n-i-p*$^+$ solar cell

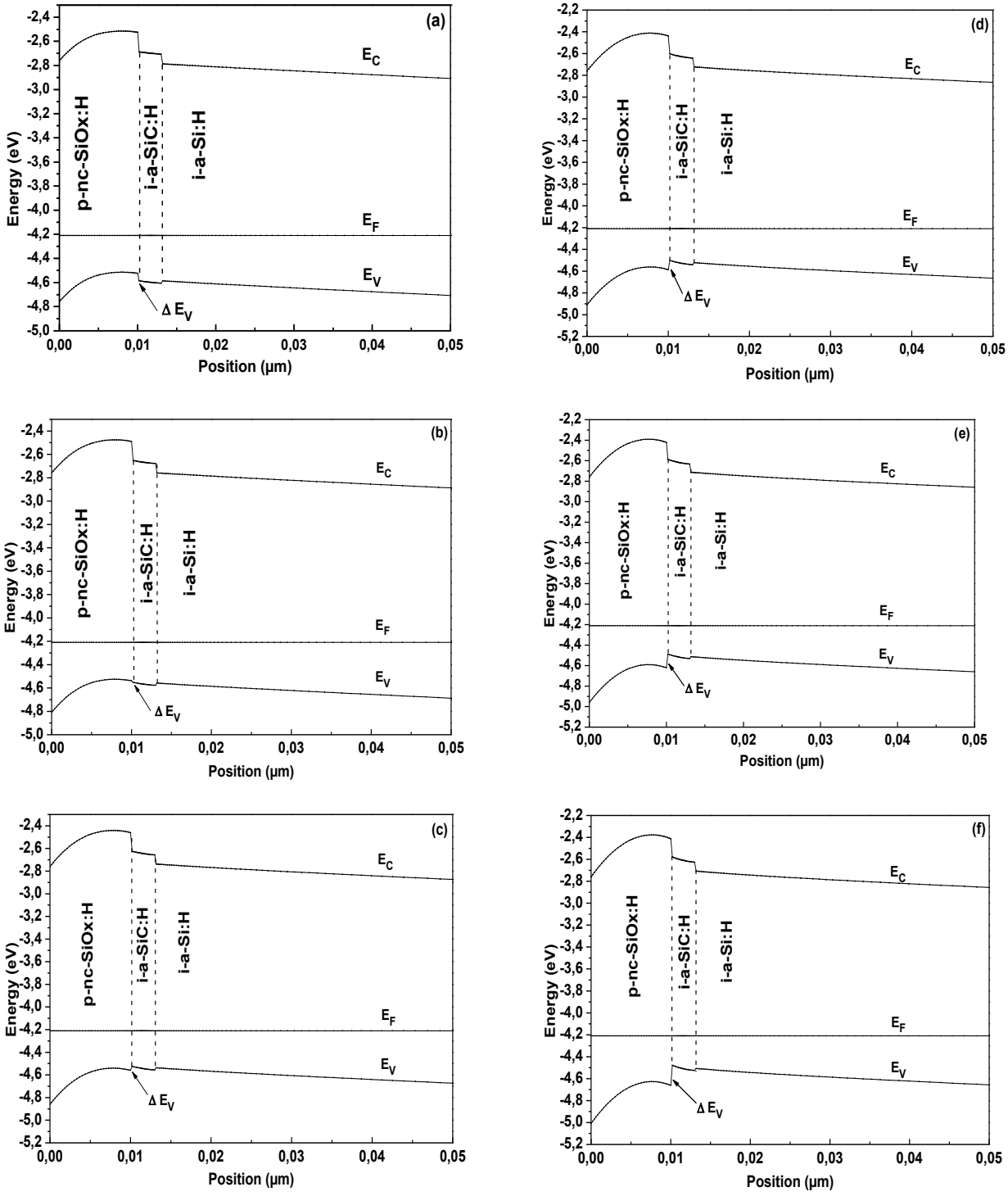

Fig. 3 – Energy band diagram of *n-i-p*$^+$ solar cells when *p-nc*-SiO*x* : H window layer band gap is (a) 2 eV ; (b) 2.05 eV; (c) 2.10 eV; (d) 2.15 eV; (e) 2.20 eV and (f) 2.25

of p^+ window, *i-a*-SiC : H buffer and *n* layer band gaps where kept as 2.10 eV, 1.90 eV and 1.75 eV, respectively. The thicknesses of p^+ layer, buffer layer, absorber layer and *n* layer were kept as 10 nm, 3 nm, 550 nm and 10 nm, respectively. Fig. 4a-d shows the variations of J_{SC}, V_{OC}, *FF* and efficiency with *i-a*-Si : H absorber layer band gap. From Fig. 4a J_{SC} was found decreased slowly from 12.20 mA/cm^2 to 11.80 mA/cm^2 with the increasing *i-a*-Si : H band gap from 1.78 eV to 1.86 eV. However, beyond 1.86 eV J_{SC} was found decreased drastically from 11.80 mA/cm^2 to 10.70 mA/cm^2.

In order to understand the decrease in value of J_{SC} with the increasing *i-a*-Si : H band gap, we explained the interaction of incoming light with material in terms of light energy ($h\nu$) and material band gap (E_g).

Upon interaction of light with material, three following cases are possible : (i) when $h\nu < E_g$, in this case no light should absorb and it transmit through the materi-

al; (ii) when $h\nu = E_g$, in this case all light should absorb and give rise to generation of maximum quantity of *e-h* pairs without a heat loss; and (iii) when $h\nu > E_g$, in this case though light will absorb but amount of light that have energy higher than band gap of material may leads to heat loss [15, 16]. This explains why as soon as the band gap of *i-a*-Si : H was increased, absorption of light having energy less than band gap was reduced. This leads to generation of less *e-h* pairs and hence, reduction in the value of J_{SC} was observed.

From Fig. 4b, it is clear that the value of V_{OC} is continuously increase from 980 mV to 1076 mV with the increasing *i-a*-Si : H layer band gap from 1.78 eV to 1.90 eV.

The increase in V_{OC} with the increasing *i-a*-Si : H layer band gap is due to the reduction of the values of band offset (ΔE_V) in valence band at *i-a*-SiC : H / *i-a*-Si : H and at *i-a*-SiC : H / p^+-*nc*-SiO*x* : H intefaces. The variations of *FF* with *i-a*-Si : H layer band gap where presented in Fig. 4c. Initially value of *FF* was increased from 0.817 to 0.829 with the increasing *i-a*-Si : H layer band gap from 1.78 eV to 1.86 eV. However beyond 1.86 eV, value of *FF* was found to decrease gradually from 0.829 to 0.816. The simulated value of efficiency showed in Fig. 4d, was found to gradually increase with the increasing *i-a*-Si : H layer band gap and reaches a maximum value of 10.44 % when band gap becomes 1.86 eV. However, beyond 1.86 eV value of efficiency decreased from 10.44 % to 10 %. Hence, *i-a*-Si : H absorber layer band gap of 1.86 eV was optimized for obtaining high efficieny for *n-i-p*$^+$ solar cell.

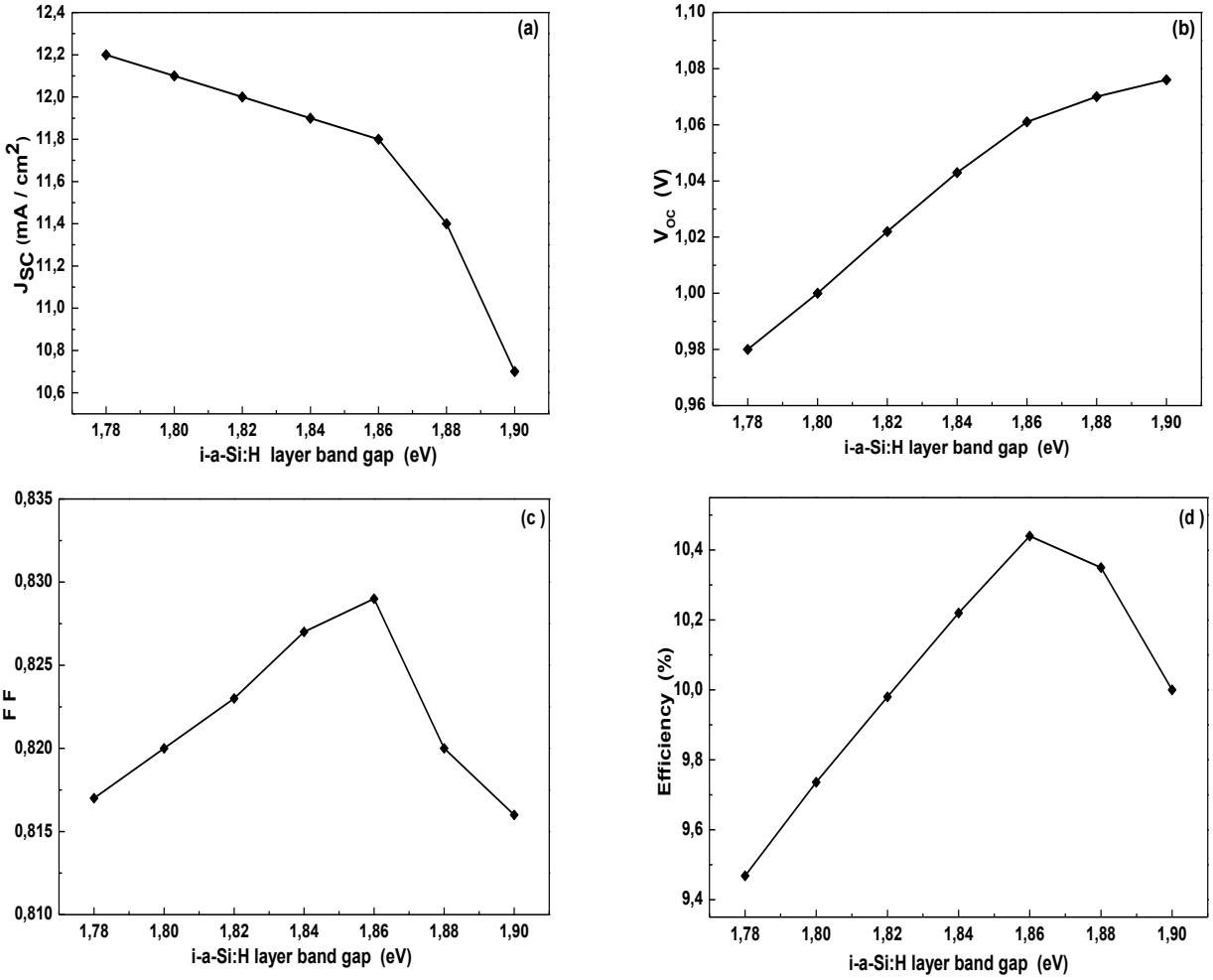

Fig. 4 – Variations of (a) J_{SC}, (b) V_{OC}, (c) *FF* and (d) efficiency with *i-a*-Si : H absorber layer band gap for *n-i-p*$^+$ solar cell

The conversion efficiency (E_{ff}) of a solar cell can be written as:

$$E_{ff} = \frac{J_{sc} V_{oc} FF}{P_{in}}, \qquad (6)$$

where P_{in} is the incident power per unit area.

According to Eq. (6), the efficiency increases with increasing the band gap of *i-a*-Si : H absorber layer from 1.78 eV to 1.86 eV is due essentially to the simultaneous increases of the V_{OC} and the *FF*. But, after 1.86 eV the decreases of efficiency is due essentially to the drastically decreases of J_{SC}.

6. CONCLUSIONS

We have simulated a *n-i-p*$^+$ solar cell by using the AMPS-1D code. Our objective, was to determine the simultaneous variation of the *i-a*-Si : H absorber layer thickness and the band gap of the p-nc-SiOx:H window

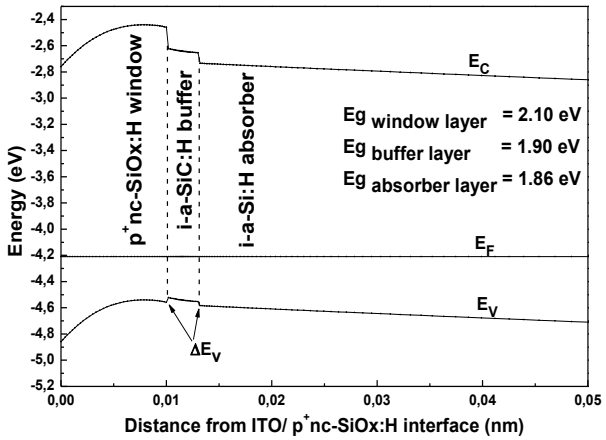

Fig. 5 – Energy band diagram of n-i-p^+ solar cells when p-nc-SiOx : H window layer band gap is 2.10 eV, i-a-SiC : H buffer layer band gap is 1.90 eV and i-a-Si : H absorber layer band gap is 1.86 eV

layer on the external performances of the solar cell. Also, the band gap of the i-a-Si : H active layer was optimized. In one hand, the simulation results shows that the J_{SC} does not depend on the p-nc-SiOx : H window layer band gap. But, J_{SC} depend strongly on the band gap and thickness of the absorber layer. On the other hand, the V_{OC} was found not more affected by the thickness of the absorber layer. However, the V_{OC} depend strongly on the band offset (ΔE_V) in valence band at i-a-SiC : H / $p^+$$nc$-SiO$x$: H interface with increasing of $p^+$$nc$-SiO$x$: H layer band gap and at i-a-SiC : H / i-a-Si : H interface, with increasing of i-a-Si : H layer band gap. Finally, it is demonstrated that the efficiency reaches a maximum value of 10.44 % (J_{SC} = 11.67 mA/cm^2; FF = 0.829; V_{OC} = 1070 mV) when values of p-nc-SiOx : H window layer band gap, band gap and thickness of i-a-Si:H absorber layer are 2.10 eV, 1.86 eV, 550 nm, respectively.

ACKNOWLEDGEMENTS

The authors are grateful to Professor S. Fonash from the Pennsylvania State University for providing the AMPS-1D program used in this study.

REFERENCES

1. R. Biron, P. Celine, F.-J. Haug, J. Escarre, K. Soderstrom, C. Ballif, *J. Appl. Phys.* **110**, 124511 (2011).
2. B. Yan, L. Zhao, J. Chen, H. Diao, G. Wang, Y. Mao, W. Wang, *J. Non-Crystal. Solids* **358**, 3243 (2012).
3. A. Belfar, H. Ait Kaci, *Thin Solid Films* **525**, 167 (2012).
4. A. Belfar, H. Ait Kaci, *Mater. Sci. Eng. B* **178**, 438 (2013).
5. L. Guo, J. Ding, J. Yang, Z. Ling, G. Cheng, N. Yuan, S. Wang, *Vacuum* **85**, 649 (2011).
6. R. Biron, P. Celine, F.-J. Haug, C. Ballif, *J. Non-Crystal. Solids* **358**, 1958 (2011).
7. N. Pingate, D. Yotsaksri, P. Sichanugrist, *Conference Record of the IEEE 4th World Conference on Photovoltaic Energy Conversion,* 1507 (2006).
8. P. Cuony, M. Marending, D.T.L. Alexander, M. Boccard, G. Bugnon, M. Despeisse, C. Ballif, *Appl. Phys. Lett.* **97**, 213502 (2010).
9. S. Fonash, J. Arch, J. Hou, W. Howland, P. Mcelheny, A. Moquin, M. Rogosky, T. Tran, H. Zhu, F. Rubinelli, *A Manual for AMPS-1D for windows 95/NT a One-Dimensional Device Simulation Program for the Analysis of Microelectronic and Photonic Structures* (The Pennsylvania State University: 1997).
10. M.I. Kabir, S.A. Shahahmadi, V. Lim, S. Zaidi, K. Sopian, N. Amin, *Int. J. Photoenerg.* **2012**, ID 460919 (2012).
11. H. Norberto, M. Arturo, *Sol. Energ. Mater. Sol. C.* **94**, 62 (2010).
12. J.K. Arch, F.A. Rubinelli, J.Y. Hou, S.J. Fonash, *J. Appl. Phys.* **69**, 7057 (1991).
13. U. Dutta, P. Chatterjee, *J. Appl. Phys.* **96**, 2261 (2004).
14. M. Zeman, et al., *Sol. Energ. Mater. Sol. C.* **46**, 81 (1997).
15. N. Dwivedi, S. Kumar, H.K. Malik, *J. Appl. Phys.* **111**, 014908 (2012).
16. M. Sharma, S. Kumar, N. Dwivedi, S. Juneja, A.K. Gupta, S. Sudhakar, K. Patel, *Sol. Energ.* **97**, 176 (2013).